Supporting Information

for

Hierarchical Nanostructures with Unique Y-shape Interconnection Networks in Manganese Substituted Cobalt Oxides: Enhancement Effect on Electrochemical Sensing Performance

By Wen-Jie Lan, Cheng-Chi Kuo, Chun-Hu Chen*

Department of Chemistry, National Sun Yat-sen University, Kaohsiung, Taiwan 80424

Center for Nanoscience and Nanotechnology, National Sun Yat-sen University, Kaohsiung, Taiwan 80424

Synthesis

The mixture of 8.08 mmol of $CoSO_4 \cdot 7H_2O$ and 2.69 mmol of $KMnO_4$ was dissolved in 71 mL D.I. water to form a purple solution with pH values lower than one. The solution was transferred to a 125 mL Teflon-lined autoclave for hydrothermal treatment at the reaction temperatures varied from 100^oC to 200^oC for 24 hours. The resulting black products were washed several times with D.I. water and then dried at $60˚C$ for 12 hours to obtain **CMOH** materials. In the experiments with various Mn substitution levels, the amount of cobalt precursor remained the same (8.08 mmol) with the change of the amount of $KMnO_4$ dissolved in the reaction mixture. For the preparation of chromium substituted cobalt oxide samples, the $KMnO_4$ was replaced with K_2CrO_4 (2.02 mmol) and followed the same experimental procedure above.

Characterization

The XRD patterns were obtained using a Bruker D8 Advance diffractometer with a CuKα X–ray source. The SEM studies were carried out using a Zeiss Supra 55 Gemini FE-SEM with at 1 kV. High-resolution TEM images were obtained in a JEOL TEM-3010 at 300kV. The BET surface area was measured with a Micromeritics ASPS 2010 system. The materials were digested with a

mixture of HCl and H_2O_2 (1:10) for elemental analysis conducted with inductively coupled plasma-mass spectroscopy (ICP-MS) analysis on a PE-SCIEX ELAN 6100 DRC. The XPS data were acquired on a Kratos Axis Ultra DLD with a Mg/Al achromatic source. To prepare the electrodes for electrochemical experiments, a homogeneous mixture of 0.001 g of samples and 1 mL ethanol was obtained first. A drop of 10 uL from this mixture was placed on the surface (0.07 cm^2) of a glassy carbon electrode and dried for 10 minutes. A Nafion (0.1%) drop with 10 uL was deposited on top of the dried samples to obtain the modified electrodes. For the H_2O_2 sensing experiments, a certain volume of H_2O_2 solution with various concentrations was injected into a 0.01M phosphate buffer solution (PBS) at pH = 7.4. Electrochemical measurements were conducted with a CHI 614D electrochemical analyzer. A conventional three-electrode configuration with Ag/AgCl (saturate NaCl) as the reference electrode and Pt as the counter electrode was used.

Figure S-1. The elemental distribution analyses of **CMOH** samples. The results of elemental mapping of Co and Mn, shown in (b) and (c) respectively, demonstrate a homogeneous distribution of these two elements in **CMOH**. The line scan results in (d), corresponding to the white dash arrow in (a), also indicate a homogeneous elemental distribution of Co/Mn with a small variation in **CMOH**.
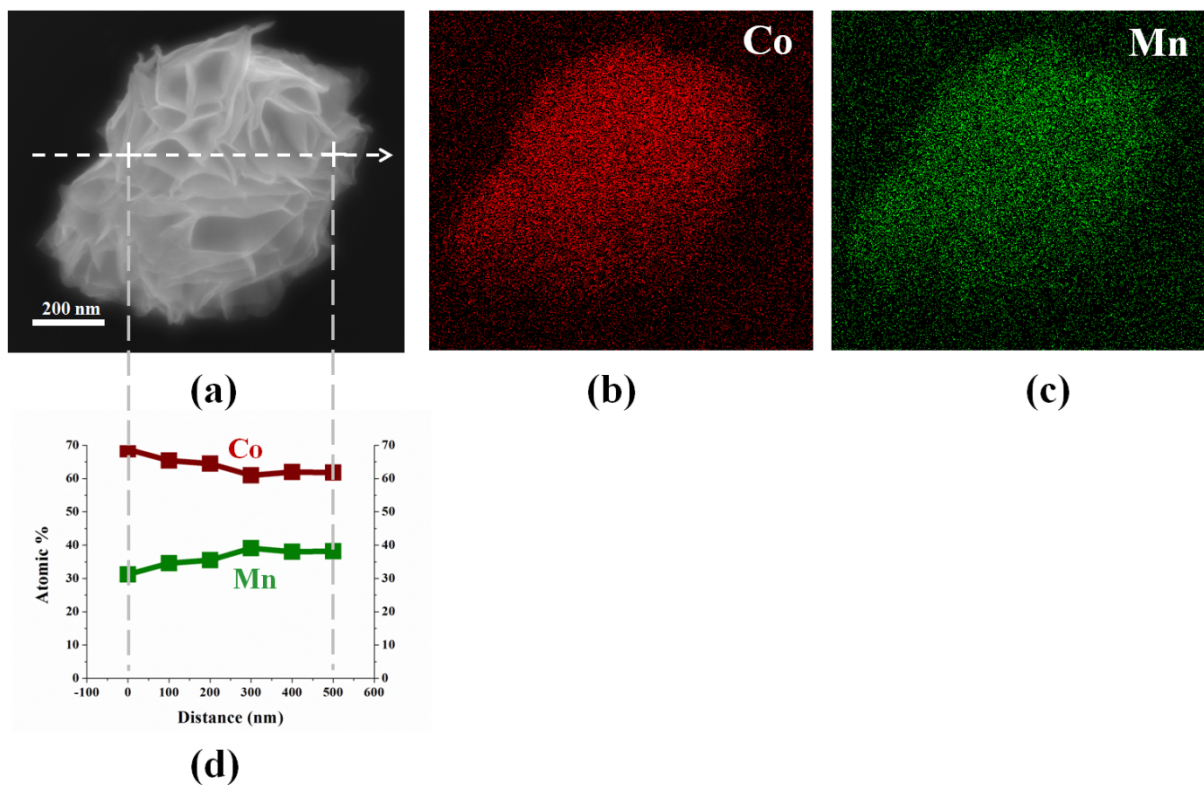
Figure S-2: The time-dependent studies of the growth processes of flower-like **CMOH** nanomaterials: (a) 0.5 hr, (b) 1 hr, (c) 2 hr, (d) 4 hr, and (e) 8 hr. All the images were taken with the same magnification.
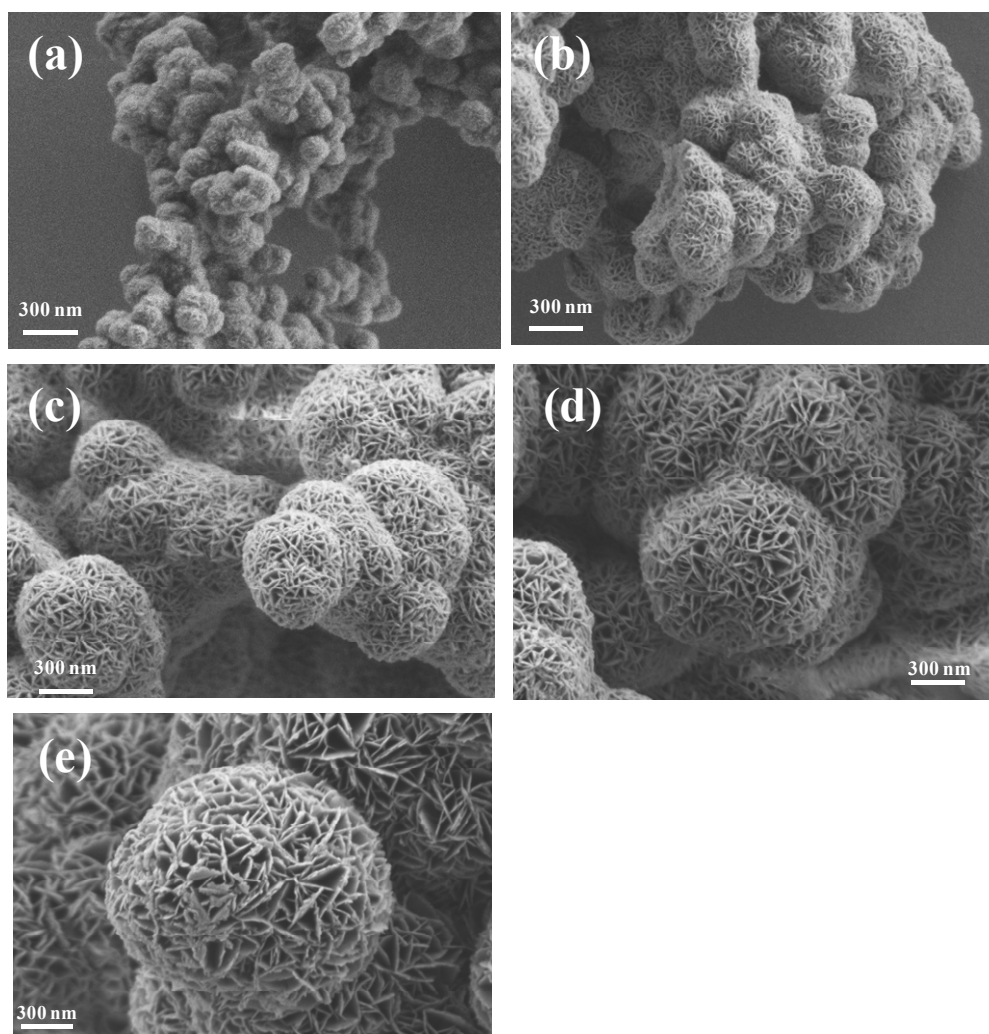
Figure S-3: The XRD patterns of the **CMOH** products in the time-dependent studies: (a) 0.5 hr, (b) 1 hr, (c) 2 hr, (d) 4 hr, (e) 8 hr, and (F) 24 hr. All the patterns correspond to CoOOH structure.
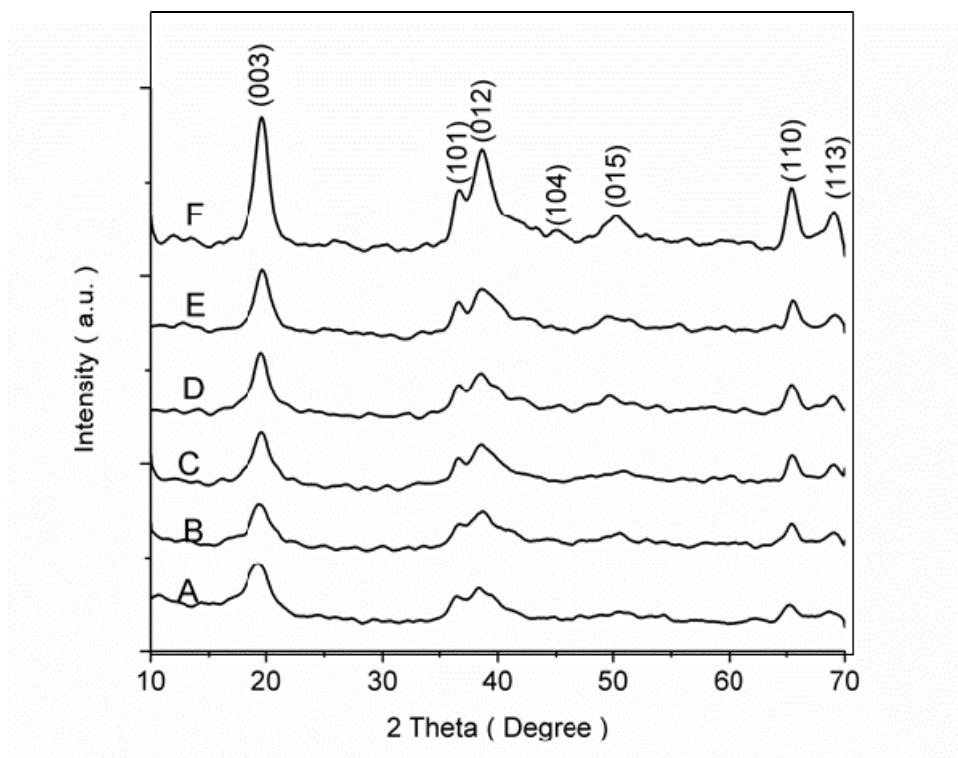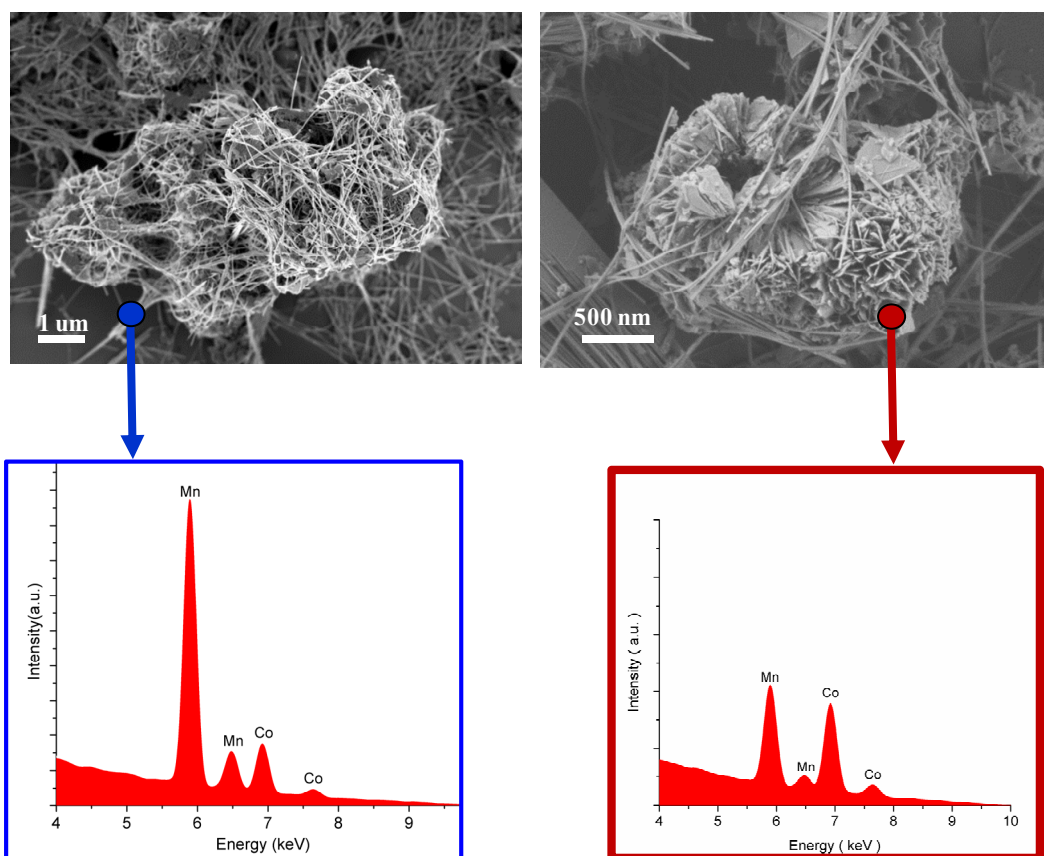
Figure S-4: The EDXS results of nanowires (same as Fig. 3e) and microspheres (same as Fig. 3f) in **CMOH** prepared at 200°C. The results show that nanowires have much higher Mn content than that of microspheres.

Table S-1. The comparison of specific surface area of **CMOH** and **CMO** materials.

Samples	Crystal Phase	Surface Area (m^2/g)	Increase of Surface Area $(\%)^b$
CMOH $(4:1)^a$	CoOOH	41.50	-
CMO $(4:1)^a$	Co_3O_4	57.77	39%
CMOH $(3:1)^a$	CoOOH	38.71	-
CMO $(3:1)^a$	Co_3O_4	53.34	38%

^{a}The Co:Mn ratios of precursors in the preparation procedure

^{b}The increase percents of surface area (**SA**) are calculated as the following: $\frac{SA_{CMO} - SA_{CMOH}}{SA_{CMOH}} \times 100\%$

Figure S-5. The comparison of calibration curves of 0.5-hour **CMO** and commercial Co_3O_4. Together with Fig. 3b, the sensitivities (slopes in the plots) of **CMO** samples are generally better than that of the commercial Co_3O_4.

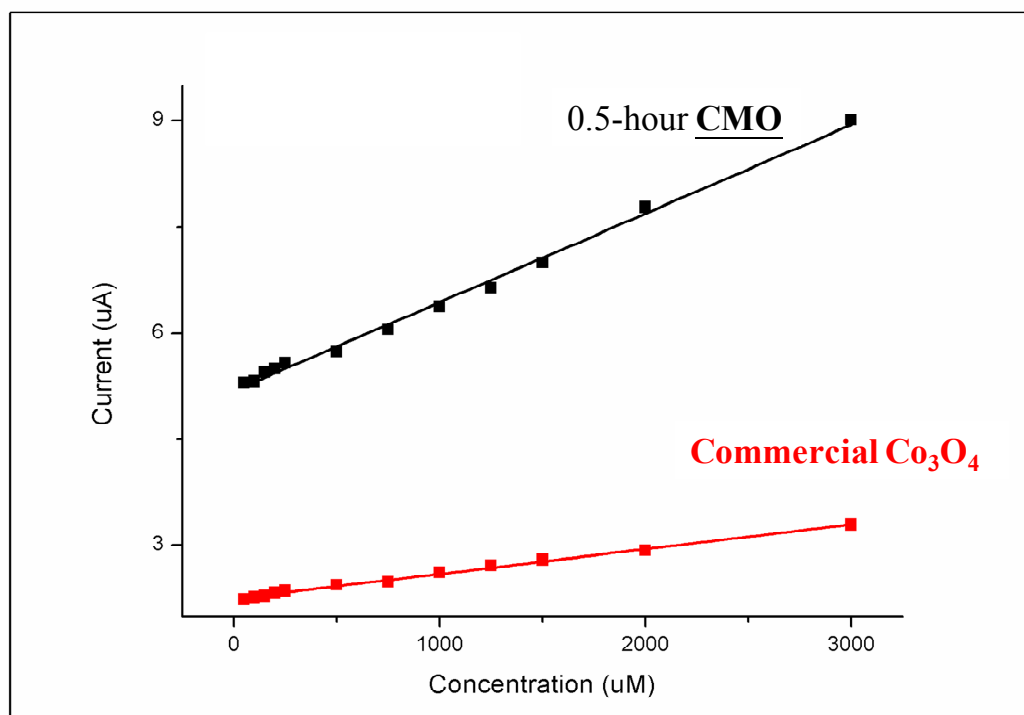Table S-2. The elemental analyses of **CMOH** prepared with various Co-to-Mn precursor ratios.

Samples	ICP-MS (Co/Mn)	EDXS (Co/Mn)
CMOH (3:1)[a]	2.39	2.33
CMOH (4:1)[a]	2.66	2.62
CMOH (6:1)[a]	2.78	2.74
CMOH (10:1)[a]	2.99	2.95

[a]The Co:Mn ratios of precursors in the preparation procedure

Figure S-6: The XPS spectra of Co 2p and and Mn 2p in **CMOH**. The binding energy (BE) values of Co 2p $_{3/2}$ and Co 2p $_{1/2}$ are 781.1 and 796.2 eV, respectively, together with the satellite signal at 790.8 eV, corresponding to Co^{3+} state.[1, 2] The BE values of Mn 2p$_{3/2}$ and Mn 2p$_{1/2}$ are 642.5 and 654.2 eV, respectively. These values are essentially identical to the Mn (IV) in the literature.[3]
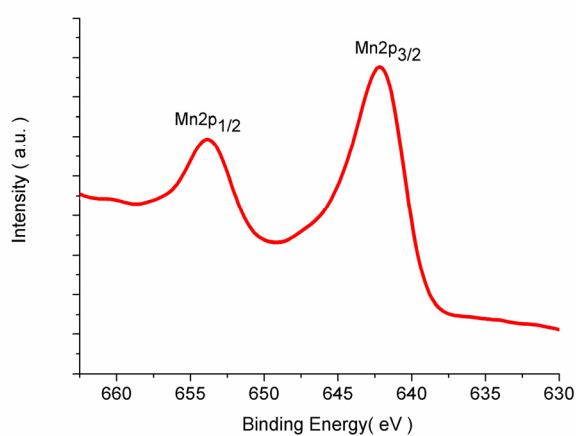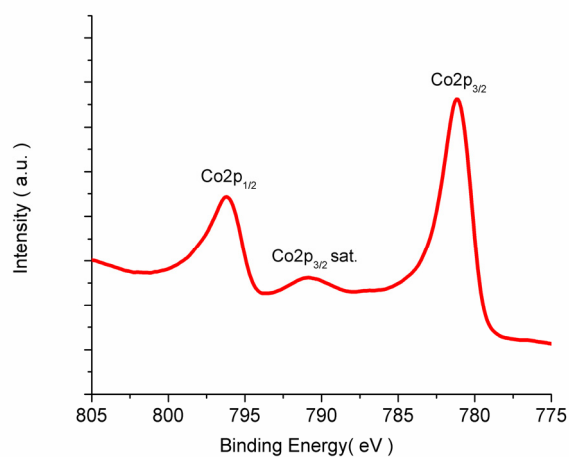
Figure S-7: The characterization results of cobalt chromium oxide. (a, b) The SEM images show a spherical assembly (400-500 nm diameters) with the flake-like nanoparticles. (c) The XRD patterns correspond to the CoOOH structure as well. (d) The EDXS results confirm the presence of Cr in the finial products. These results provide the additional evidence for the generality of redox process toward the controlled synthesis of substituted nanomaterials.
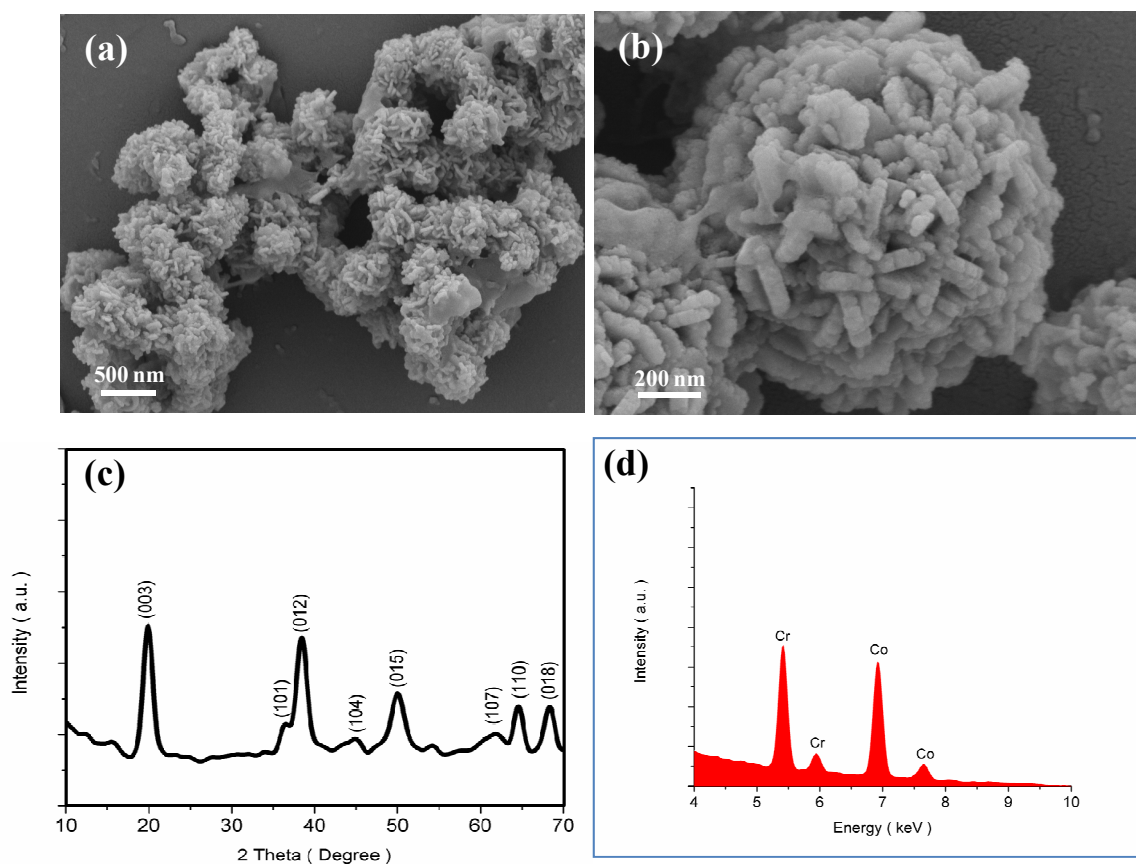
Reference

1. J. Yang, H. Liu, W. N. Martens and R. L. Frost, *J. Phys. Chem. C*, 2010, **114**, 111.

2. J. C. CARVER and G. K. SCHWEITZER, *J. Chem. Phys.*, 1972, **57**, 973.

3. X.-S. Liu, Z.-N. Jin, J.-Q. Lu, X.-X. Wang and M.-F. Luo, *Chem. Eng. J.*, 2010, **162**, 151-157.